DOI 10.1016/j.arbres.2023.01.012

CC BY NC ND

Antifibrotic Effects of Extracellular Vesicles from Umbilical Cord-Mesenchymal Stem Cells on Lung Myofibroblast Cells.

Idiopathic pulmonary fibrosis (IPF) is a chronic fibroproliferative disease characterized by a progressive and irreversible lung scaring with a decline in lung function[1]. Transforming Grow Factor Beta (TGF-β) induced myofibroblasts[2] are considered as key cells in this pathology, which are responsible of the aberrant fibrosis[3]. Recently, mesenchymal stem cells (MSCs) treatment has demonstrated a regenerative effect[4,5] and their extracellular vesicles (EVs) have been established as one of their main therapeutic components[6,7]. Thus, EVs administration as a biological therapy overcomes the drawbacks of cell transplantation[8]. Here, we evaluated the potential anti-fibrotic effects of EVs isolated from human umbilical cord MSCs (hUC-MSCs) in a model of lung myofibroblasts[9].

First, we established an *in vitro* primary model of myofibroblasts from Lung MSCs (L-MSCs) through TGF-β1 priming. Lung tissues were obtained from donors without history of lung disease (n=3) and with IPF (n=3) under the approval of the ethical committee of Balearic Islands (Code: IB745/06PI). L-MSCs were obtained using previously described methods[10], and their mesenchymality was confirmed by Rohart test[11]; cells were induced to myofibroblasts with 5ng/ml TGF-β1 for 24 h[9].

Second, we obtained human Umbilical Cord MSCs (hUC-MSCs) from the IdISBa Biobank. hUC-MSCs were growth in media supplemented with 10 % of platelet lisate (PL) until 80 % confluence. Then, cells were washed twice with PBS and cultured with medium without PL (DMEM low glucose supplemented with 2% P/S) for 48 h. This conditioned media was employed for EVs isolation by size exclusion chromatography (SEC), followed by ultrafiltration[12]. Next, EVs were characterized by Size, Morphology and Biomarker expression (Figure 1A, 1B and 1C) by Western Blot (WB), , Transmission

DOI 10.1016/j.arbres.2023.01.012
CC BY NC ND

Electronic Microscopy (TEM) and Nanoparticle Tracking Analysis (NTA) as previously described[12]. For EVs treatment, we set two concentrations of EVs (12 and 60 ug/ml) obtained by absorbance at 280 nm using a NanoDrop; these concentrations corresponded to $3x10^{10}$ and $1.5x10^{11}$ particles/ml by NTA respectively.

Then, we treated Myofibroblasts from non-fibrotic L-MSCs during 24 h to determine expression of fibrotic related gene. This analysis showed not significant differences in ACTA2, Col1A1, TGF-β1, END1 and TIMP1. However, a significant dose-dependent increase on *MMP1* mRNA expression (Figure 1D), confirmed by increased MMP1 protein levels (measured by ELISA) released to culture media at 72 and 144 h after treatment for the higher dose (60 µg/ml) of EVs (Figure 1E). In this line, a significant reduction of collagen deposits (stained with Sirius Red and quantified at 540 nm[13]) was observed in cells treated with the higher EVs concentration for 144 h (Figure 1F). Next, we performed a Presto Blue assay according to manufacturer's instructions (Life Technologies, CA, USA) to evaluate cell viability and a LDH activity according to manufacturer's protocol (Roche Diagnostics, Manheim, Germany) to evaluate cytotoxicity as other possible causes of collagen reduction. The obtained results indicate that the collagen reduction induced by the high dose EVs treatment was accompanied by a significant decrease on cell viability and increased cell cytotoxicity at 72 and 144 h (Figures 1G and 1H). Though, this effect was not observed if cells were not previously primed with TGF-β1.

Then, to evaluate the translational importance of our findings, we obtained TGF-β1 induced myofibroblasts from MSCs of IPF lung tissues. We treated them with EVs derived from hUC-MSCs, as previously described. As seen in Figure 2, treatment with EVs induced the same effects on cells derived from IPF patients. A significant reduction on collagen deposits and on cell viability was observed when cells were primed with

DOI 10.1016/j.arbres.2023.01.012
CC BY NC ND

TGF-β1 (Figure 2A and 2B) as well as a significant increase on released LDH and MMP1 to cell culture media when cells were treated with the highest EVs concentration (60 µg/ml) (Figure 2C and 2D). It is important to highlight that, in any case, EVs do not produce significant differences in L-MSCs if cells are not previously primed with TGF-β1 in both, healthy and pathological lung originated cells, in all the experiments performed until now.

Thus, we next investigated the proteomic signatures and, therefore, activation of different signalling routes induced by EVs treatment in L-MSCs being or not previously primed with TGF-β1. We performed an experiment that included 4 groups: non treated L-MSCs, non TGF-β1 primed L-MSCs + 12 ng/ml EVs, TGF-β primed L-MSCs without EVs treatment and TGF-β1 primed L-MSCs + 12 ng/ml EVs. After an overnight incubation, cells were lysed and analysed by Reverse Phase Protein Array (RPPA) at the proteomic facilities of MDAnderson cancer centre (Dallas, USA) according with their protocols[14]. This analysis demonstrated that there are several proteins differentially expressed for each kind of treatment and 13 proteins differentially expressed in EVs treated fibrotic cells as shown in the VENN diagram (Figure 2E). Confirming a specific signature on EVs treated myofibroblasts. Additionally, in the same groups of cells, we evaluated Autophagy after 72 h of EVs treatment by identification of microtubule-associated proteins 1A/1B light chain 3B (LC3B (NB100-2220 NOVUS, Colorado, USA)) using Immune Fluorescence (IF) to identify auto-phagosomes. We observed an increased number of autophagosomes in TGF-β1 primed L-MSCs treated for 72 h with 12 ug/ml EVs (Figure 8 A). Finally, we wanted to know if EVs induce cell death and apoptosis in TGF-β1 primed cells. Thus, at 72 h of EVs treatment we performed Annexin V and Propidium Iodide analysis by flow cytometry, using the apoptosis AnnexinV kit (AbCam Cambridge, UK), following the supplier recommendations. In fact, we observed a significant increase of AnnexinV

DOI 10.1016/j.arbres.2023.01.012
CC BY NC ND

positive cells on TGF-β1 primed cells when treated with EVs compared with the other groups in both, cells obtained from healthy donors (87.47 % vs 54.07 %) and cells obtained from IPF donors (87.07 % vs 50.53 %). Showing the same pattern for PI positive cells (7.23 % vs 3.23 % in cells from healthy donors and 6.81 % vs 3.64 % in IPF donors). These results are in agreement with the reduced cell viability observed in cells treated with EVs that have previously been primed with TGF-β1.

Summarizing, in this work we have showed that EVs from hUC-MSCs generate a specific modulation of myofibroblasts originated by priming MSCs with TGF-β1 obtained from both, normal and pathological lungs. This myofibroblasts are part of the fibroblastic loci and responsible of the excessive deposition of disorganised collagen and extracellular matrix, all in all resulting in the distortion of the normal lung architecture[2,15]. Here, we have showed that EVs treatment produce a reduction of collagen deposits, an increase of collagenase MMP1 and a reduction of myofibroblasts cell viability with increased autophagy and apoptosis. Although nowadays, its clinical translation still needs improvement on EVs production process and determining the best administration via; our findings increase the scientific evidence for the use of EVs as treatment in fibrosis diseases, representing a hope for IPF treatment.

References:

1. Plantier L, Cazes A, Dinh-Xuan AT, Bancal C, Marchand-Adam S, Crestani B. Physiology of the lung in idiopathic pulmonary fibrosis. *Eur Respir Rev*. 2018;27(147). doi:10.1183/16000617.0062-2017

2. Eickelberg O, Köhler E, Reichenberger F, et al. Extracellular matrix deposition by primary human lung fibroblasts in response to TGF-β1 and TGF-β3. *Am J Physiol Cell Mol Physiol*. 1999;276(5):L814-L824. doi:10.1152/ajplung.1999.276.5.L814

3. Kulkarni T, O'Reilly P, Antony VB, Gaggar A, Thannickal VJ. Matrix remodeling in pulmonary fibrosis and emphysema. *Am J Respir Cell Mol Biol*. 2016;54(6):751-760. doi:10.1165/rcmb.2015-0166PS

4. Guillamat-Prats R. The Role of MSC in Wound Healing, Scarring and Regeneration. *Cells*. 2021;10(7). doi:10.3390/CELLS10071729

DOI 10.1016/j.arbres.2023.01.012

5. Bandeira E, Oliveira H, Silva JD, et al. Therapeutic effects of adipose-tissue-derived mesenchymal stromal cells and their extracellular vesicles in experimental silicosis. *Respir Res*. 2018;19(1):104. doi:10.1186/s12931-018-0802-3

6. Kubo H. Extracellular Vesicles in Lung Disease. *Chest*. 2018;153(1):210-216. doi:10.1016/j.chest.2017.06.026

7. Grange C, Tritta S, Tapparo M, et al. Stem cell-derived extracellular vesicles inhibit and revert fibrosis progression in a mouse model of diabetic nephropathy. *Sci Rep*. 2019;9(1):1-13. doi:10.1038/s41598-019-41100-9

8. Reis M, Mavin E, Nicholson L, Green K, Dickinson AM, Wang X. Mesenchymal Stromal Cell-Derived Extracellular Vesicles Attenuate Dendritic Cell Maturation and Function. *Front Immunol*. 2018;9(NOV):2538. doi:10.3389/fimmu.2018.02538

9. Evans RA, Tian YC, Steadman R, Phillips AO. TGF-β1-mediated fibroblast-myofibroblast terminal differentiation - The role of Smad proteins. *Exp Cell Res*. 2003;282(2):90-100. doi:10.1016/S0014-4827(02)00015-0

10. Rolandsson S, Andersson Sjöland A, Brune JC, et al. Primary mesenchymal stem cells in human transplanted lungs are CD90/CD105 perivascularly located tissue-resident cells. *BMJ Open Respir Res*. 2014;1(1). doi:10.1136/bmjresp-2014-000027

11. Rohart F, Mason EA, Matigian N, et al. A molecular classification of human mesenchymal stromal cells. *PeerJ*. 2016;2016(3). doi:10.7717/peerj.1845

12. Ortega FG, Roefs MT, de Miguel Perez D, et al. Interfering with endolysosomal trafficking enhances release of bioactive exosomes. *Nanomedicine Nanotechnology, Biol Med*. 2019;20. doi:10.1016/j.nano.2019.102014

13. Lattouf R, Younes R, Lutomski D, et al. Picrosirius Red Staining: A Useful Tool to Appraise Collagen Networks in Normal and Pathological Tissues. *J Histochem Cytochem*. 2014;62(10):751-758. doi:10.1369/0022155414545787/ASSET/IMAGES/LARGE/10.1369_0022155414545787-FIG2.JPEG

14. Siwak DR, Li J, Akbani R, Liang H, Lu Y. Analytical Platforms 3: Processing Samples via the RPPA Pipeline to Generate Large-Scale Data for Clinical Studies. In: *Advances in Experimental Medicine and Biology*. Vol 1188. Springer; 2019:113-147. doi:10.1007/978-981-32-9755-5_7

15. Barkauskas CE, Noble PW. Cellular Mechanisms of Tissue Fibrosis. 7. New insights into the cellular mechanisms of pulmonary fibrosis. *Am J Physiol - Cell Physiol*. 2014;306(11):C987. doi:10.1152/ajpcell.00321.2013

Figure Captions

Figure 1. EVs Characterization and effect in myofibroblast from non-fibrotic lungs.

hUC-MSCs culture supernatant was concentrated to 5 ml by tangential flow filtration and immediately injected into a SEC column and fractioned in 5 ml fractions. ***(A)*** Presence of specific EVs markers (HSC70 (clone B-6, Santa Cruz, USA) and CD81 (clone B-11, Santa Cruz, USA)) and lack of GM130 (clone N3C2, Santa Cruz, USA)

DOI 10.1016/j.arbres.2023.01.012
CC BY NC ND

evaluated *by WB in the collected fractions. Higher expression of EVs marker can be observed at fraction 8 and 9, corresponding with higher UV absorbance in the chromatogram.* ***(C)*** *Representative TEM image of isolated EVs.* ***(D)*** *NTA analysis of pulled EV enriched fractions (7-10) shows particles with 163 nm mean size.* ***(D)*** *Gene expression of fibrosis related genes. Data represent fold changes of target genes normalized to beta-actin and GAPDH (reference genes) expressed relative to control that was set to 100%.* ***(E)*** *MMP1 protein levels released to cell culture media at 0, 72 and 144 h after treatment.* ***(F)*** *Quantification of the Sirius Red stained collagen in TGF-β1 induced myofibroblasts. Data represents fold changes relative to non TGF-β1 primed cells.* ***(G)*** *Cell Viability measured after 0, 72 and 144 h of EVs treatment in TGF-β1 induced myofibroblasts. Data represent fold changes relative to non-treated TGF-β1 primed cells at each time point.* ***(H)*** *LDH activity in cell culture media after 0, 72 and 144 h of EVs treatment in TGF-β1 primed cells. Data represent fold changes relative to non-treated TGF-β1 primed cells at each time point. Values represent the mean ± S.D. Three independent experiments were performed. Multiple t student and ANOVA tests were performed to assess differences: * $p < 0.05$; ** $p < 0.005$; *** $p < 0.0005$.*

Figure 2. Effects of EV in myofibroblasts from obtained from IPF lungs.

(A) *Quantification of Sirius Red stained collagen in TGF-β1 primed cells. Data represents fold changes relative to non TGF-β1 primed cells.* ***(B)*** *Cell viability measured after 0, 72 and 144 h of EVs treatment in TGF-β1 primed cells. Data represents fold changes relative to non EVs treated cells at each time point.* ***(C)*** *LDH activity released to cell culture media after 0, 72 and 144 h of EVs treatment in TGF-β1 primed cells. Data represent fold changes relative to non EVs treated cells at each time point.* ***(D)*** *MMP1 protein levels released to cell culture media at 72 and 144 h after EVs treatment in TGF-β1 primed cells.* ***(E)*** *Proteomic analysis of 483 total and phosphorylated proteins were*

DOI 10.1016/j.arbres.2023.01.012

analysed by Reverse Phase Protein Array (RPPA) of cells from an IPF patient under 4 conditions: non treated L-MSCs, non TGF-β1 primed L-MSCs + 12 ng/ml EVs, TGF-β primed L-MSCs without EVs treatment and TGF-β1 primed L-MSCs + 12 ng/ml EVs, Venn diagram showing differentially expressed (over 0.3 Log^2 median-centered) proteins between groups. ***(F)*** *Representative confocal images of cells stained for LC3-B in green (FITC), actin in red (Phalloidin-Texas red) and nuclei in blue (DAPI).* ***(G)*** *Graphical representation of AnnexinV and Propidium Iodide positive cells at 72 h of EVs treatment. Multiple t student test and ANOVA tests were performed to assess differences between group of samples: * p < 0.05; ** p< 0.005; *** p< 0.0005.*

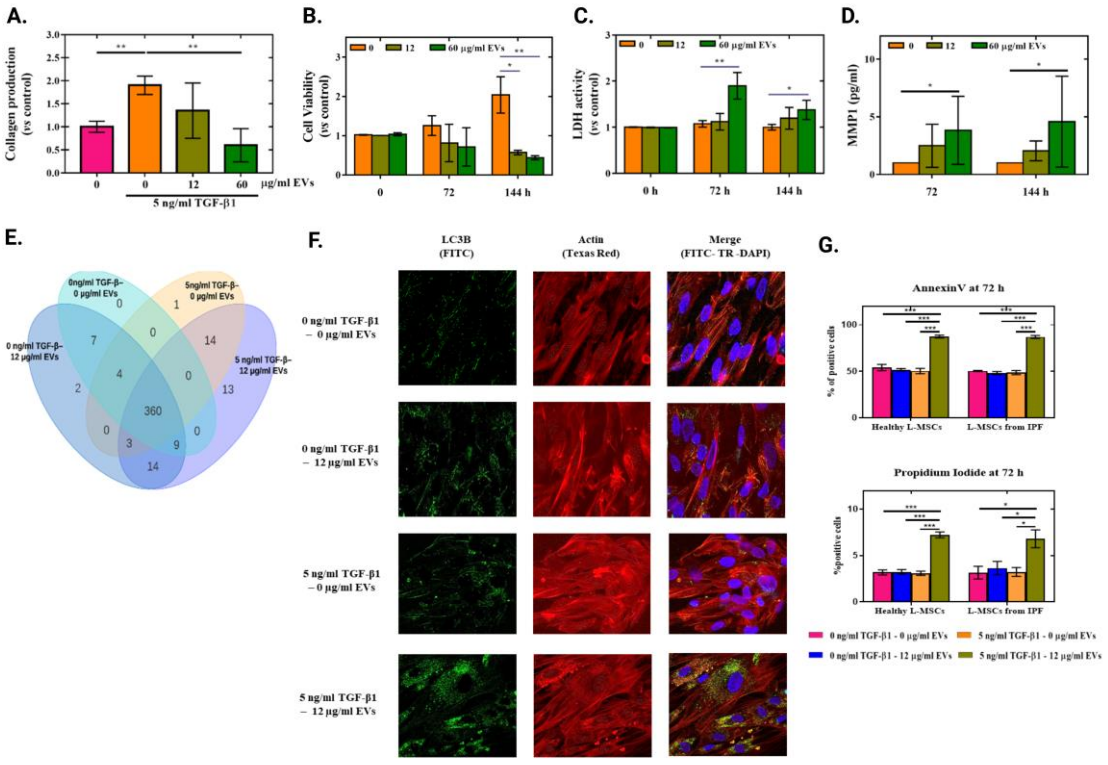

DOI 10.1016/j.arbres.2023.01.012

CC BY NC ND